FROM RESIDUAL MESOGENS TO RESPONSIVE MATERIALS: RECYCLED LIQUID CRYSTALS FROM END-OF-LIFE SCREENS IN PHOTOCURABLE ACRYLATE NETWORKS

Amina BOURICHE [1,2], Ana BARRERA[2], Corinne BINET[2], Patrick ROPA[3], Frédéric DUBOIS[3], Lamia ALACHAHER-BEDJAOUI[1], Zohra BOUBERKA[4], Monica ILIŞ[5*], Ulrich MASCHKE[2*]

Photocurable composites were developed using isobornyl acrylate and recycled liquid crystal components, cured under ultraviolet light with a reactive crosslinker and photoinitiator. Physical characterization included infrared spectroscopy, differential scanning calorimetry, dynamic mechanical analysis, and rheology. Spectroscopy confirmed over 90% conversion of carbon–carbon double bonds. Calorimetry revealed suppression of mesophase transitions, indicating effective encapsulation. Mechanical analysis showed a glass transition temperature decrease from approximately 90°C to 65°C and a marked reduction in stiffness. Rheological measurements indicated enhanced flow due to lower viscosity. These results demonstrate a plasticizing effect and compatibility of the recycled liquid crystals, enabling tunable functional properties for optical applications.

Keywords: Photopolymerization; glass transition; mesophase; storage modulus; viscosity

1. Introduction

In recent years, the recycling and valorization of electronic waste have attracted growing interest due to environmental constraints and the diminishing availability of primary resources [1–3]. Among these waste streams, end-of-life liquid crystal displays (LCDs) represent a significant source of reclaimable

[1] Laboratoire de Recherche sur les Macromolécules (LRM), Faculté des Sciences, Université Abou-bekr Belkaïd de Tlemcen (UABT), BP 119, 13000 Tlemcen, Algeria
[2] Unité Matériaux et Transformations (UMET), UMR 8207, Université de Lille, CNRS, INRAE, Centrale Lille, F-59000 Lille, France, e-mail: ulrich.maschke@univ-lille.fr
[3] Unité de Dynamique et Structure des Matériaux Moléculaires (UDSMM), UR 4476, Université du Littoral – Côte d'Opale, CS 80699, 62228 Calais, France
[4] Laboratoire Physico-Chimie des Matériaux-Catalyse et Environnement (LPCMCE), Université des Sciences et de la Technologie d'Oran Mohamed Boudiaf (USTOMB), BP 1505, El M'naouer, Oran 31000, Algeria
[5] Department of Inorganic and Organic Chemistry, Biochemistry and Catalysis, University of Bucharest, Bucharest, Romania, e-mail: monica.ilis@chimie.unibuc.ro
* corresponding authors

materials, particularly recycled liquid crystals (LCRs). These LCRs retain core mesogenic structures, such as aromatic esters and nitrile-functionalized biphenyls, which exhibit intrinsic anisotropic behavior and dielectric responsiveness [4–6]. Such properties position LCRs as promising candidates for reuse in optoelectronic, photonic, and responsive soft-matter systems [7].

Isobornyl acrylate (IBOA) is a monoacrylate monomer known for its high refractive index, excellent optical clarity, and dimensional stability under polymerization. In photocurable formulations, IBOA is often co-polymerized with multifunctional crosslinkers such as 1,6-hexanediol diacrylate (HDDA), producing dense polymer networks with enhanced rigidity and solvent resistance [8–11]. Photoinitiated free-radical polymerization, typically initiated by α-hydroxy ketone derivatives such as Darocur 1173 under ultraviolet radiation (~365 nm), enables spatial and temporal control over network formation, critical for advanced device fabrication [12].

While hybrid and bio-based acrylate systems have demonstrated compatibility with a variety of nanomaterials and molecular dopants [13–14], the incorporation of recycled LCRs into photopolymer matrices remains poorly characterized, particularly in terms of their effects on molecular dynamics, phase behavior, and mechanical moduli. Prior work on polymer-dispersed liquid crystals (PDLCs) and LC–polymer composites suggests that such mesogenic additives can act as plasticizers, internal phase modifiers, or even induce mesophase separation within the host polymer [15–17]. These behaviors are governed by complex interactions among crosslink density, mesogen orientation, and interfacial compatibility—features that can be quantified through physical characterization techniques.

In this study, we present a systematic formulation and physical characterization of UV-curable polymer networks composed of IBOA, recycled LCRs, and HDDA as a difunctional crosslinker. The evolution of molecular structure, phase transitions, and mechanical response is investigated through Fourier-transform infrared spectroscopy (FTIR), differential scanning calorimetry (DSC), dynamic mechanical analysis (DMA), and rotational rheometry. These techniques enable quantification of curing kinetics, thermal relaxation phenomena, viscoelastic moduli, and flow behavior—allowing for a detailed understanding of structure–property relationships relevant to soft matter physics and functional material design.

2. Experimental

2.1. Materials

The study utilized the monofunctional monomer isobornyl acrylate (IBOA) and the difunctional monomer 1,6-hexanediol diacrylate (HDDA). The

photoinitiator, 2-hydroxy-2-methyl-1-phenyl-propan-1-one, commonly referred to as Darocur 1173, was used in this research. All chemicals were obtained from Sigma-Aldrich (Saint Quentin Fallavier, France) and were employed without any further purification.

Recycled liquid crystals (LCRs) were sourced from discarded liquid crystal displays (LCDs). The extraction process for the LCRs is described in the references [4–6].

2.2. Sample preparation

The formulations were created by blending IBOA with 0.5 weight% (wt%) of HDDA and 0.5 wt% Darocur 1173 as the photoinitiator. LCRs were incorporated in varying concentrations to evaluate their impact on the properties of the resulting cured materials. The mixtures were thoroughly homogenized using magnetic stirring. UV curing was carried out with a mercury vapor lamp emitting at 365 nm for 50 min.

2.3. Fourier Transform Infrared Spectroscopy (FTIR)

FTIR spectra were recorded on a Bruker Alpha spectrometer (Bruker Corporation, Billerica, MA, USA), using an attenuated total reflectance (ATR) module. Spectra were collected in the range of 4000 to 400 cm^{-1} with a resolution of 4 cm^{-1}, averaging 32 scans per sample. The conversion of the acrylate groups was determined by monitoring the decrease in the characteristic C=C stretching peak near 810 cm^{-1}.

2.4. Differential Scanning Calorimetry (DSC)

Thermal properties were measured using a TA Instruments Q2000 differential scanning calorimeter (TA Instruments, New Castle, DE, USA). About 5–10 mg of each sample was placed in an aluminum pan, and a heating cycle from –70 °C to 200 °C was applied at a rate of 10 °C/min under a nitrogen atmosphere. The glass transition temperature (T_g) was identified from the midpoint of the heat capacity change.

2.5. Dynamic Mechanical Analysis (DMA)

Dynamic mechanical properties were assessed with a TA Instruments Q800 dynamic mechanical analyzer (TA Instruments, New Castle, DE, USA) in tensile mode. Rectangular specimens were tested within the temperature range of 20 °C to 150 °C, with a heating rate of 3 °C/min and a frequency of 1 Hz. The storage modulus (E′), loss modulus (E″), and damping factor (tan δ) were

measured to assess the mechanical performance and determine the glass transition temperature (T_g).

2.6. Rheological Analysis

The rheological properties of the uncured formulations were analyzed using an Anton Paar MCR 302 rheometer (Anton Paar GmbH, Graz, Austria) with a 25 mm parallel plate geometry. Measurements were carried out at 25°C under oscillatory shear mode. A frequency sweep from 0.1 to 100 rad/s was performed at a constant strain within the linear viscoelastic region. The storage modulus (G′), loss modulus (G″), and complex viscosity (η*) were recorded to examine the flow behavior and crosslinking potential of the (IBOA/HDDA/Darocur)/LCR mixtures before curing.

3. Results and discussion

3.1. Fourier-transform infrared spectroscopy analysis

The prepared monomer blends were analyzed by FTIR spectroscopy both before and after polymerization/curing. Fig. 1a presents the FTIR spectra of a 99 wt% IBOA blend comprising 0.5 wt% HDDA and 0.5 wt% Darocur 1173, recorded in both the monomeric and cured states. In the monomeric state, characteristic vibrational bands are observed. These include the asymmetric stretching vibration of methyl groups (CH_3) at 2961 cm^{-1}, a strong carbonyl (C=O) stretching band at ~1719 cm^{-1}, and a C=C stretching vibration associated with the acrylate double bond at 1637 cm^{-1}. A skeletal vibration of C–C single bonds is observable at 1175 cm^{-1}, and the out-of-plane deformation mode of the vinyl C=C bond is distinctly discernible at 810 cm^{-1}.

Following the polymerization/curing process, the positions of all functional groups remain constant; however, a significant decrease in band intensity is evident, particularly for the C=C bands. Fig. 1b shows a magnified view of the 810 cm^{-1} region, demonstrating the complete disappearance of this band after the curing process. This observation suggests that all reactive double bonds have been fully consumed, indicating the formation of a crosslinked polymer network [18-22]. The disappearance of the C=C out-of-plane bending signal, which is associated with unreacted C=C double bonds, strongly supports the efficiency of the curing process. These spectral changes are consistent with those reported in the literature for acrylate polymerization systems [12, 23-24].

This decrease in intensity, particularly of the C=C bands, correlates with the progression of the polymerization reaction and network formation. As polymerization progresses, monomeric vinyl groups (C=C) are converted into single bonds, resulting in the growth of polymer chains and the development of a

crosslinked network. The complete disappearance of the C=C band at 810 cm^{-1} indicates a high degree of monomer conversion and a well-developed network, suggesting rapid and efficient curing kinetics in the presence of the photoinitiator and HDDA crosslinker.

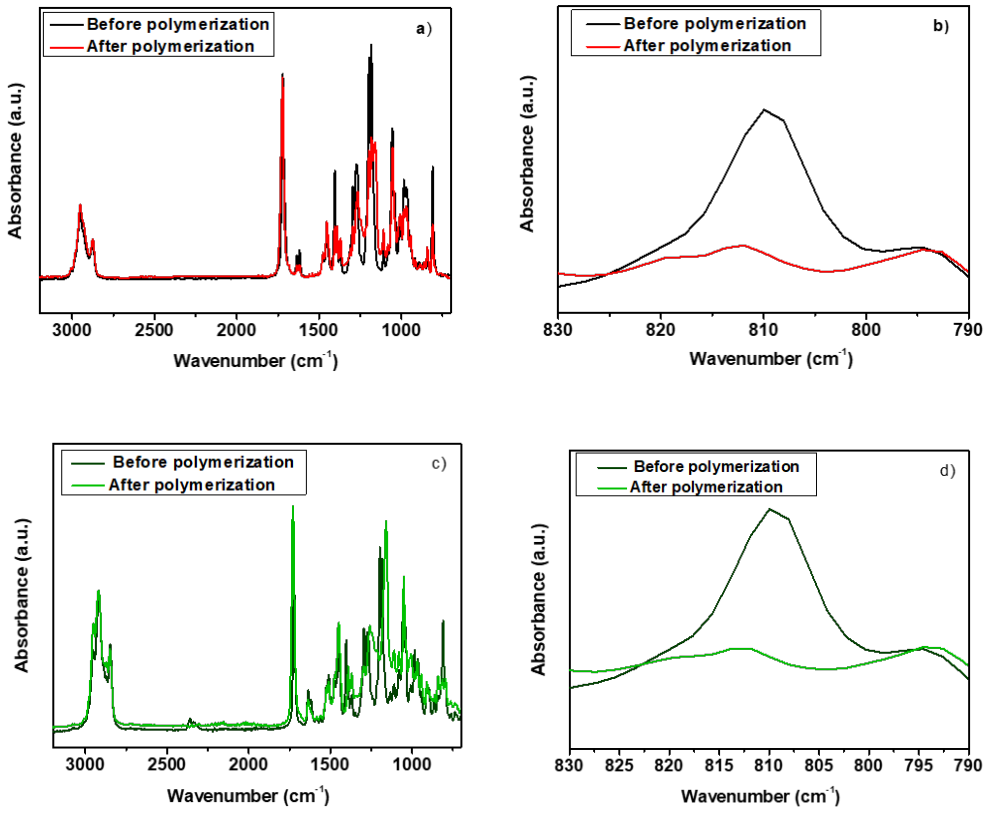

Fig. 1. FTIR spectra before and after polymerization/curing reactions : a) 100 wt % (IBOA/HDDA/Darocur), b) magnified view of a) around 810 cm^{-1}, c) 70 wt % LCR /30 wt % (IBOA/HDDA/Darocur) and d) magnified view of c) around 810 cm^{-1}.

In order to assess the impact of incorporating LCRs, Fig. 1c presents the FTIR spectra of a blend consisting of 70 wt% LCR and 30 wt% (IBOA/HDDA/Darocur), recorded before and after 50 min of polymerization. The spectral features remain consistent, and no new bands are observed, indicating that the chemical nature of the system remains constant. As was the case with the preceding formulation, peak intensities related to the reactive acrylic groups undergo a decrease following the curing process.

Fig. 1d presents a magnified perspective of the 810 cm^{-1} region depicted in Fig. 1c. The observed disappearance of the band following polymerization and subsequent curing processes serves to confirm the near-total consumption of C=C

double bonds, even in the presence of LCRs. This result suggests that the LCRs are chemically compatible with the reactive initial monomeric mixture and do not interfere with the photoinitiated polymerization process or the formation of the crosslinked polymer network.

3.2. Differential Scanning Calorimetry analysis

DSC thermograms of poly(IBOA/HDDA/Darocur) and LCRs are shown in Fig. 2. The LCRs exhibit a smectic-to-nematic phase transition ($T_{S–N}$) at approximately –46.6 °C and a nematic-to-isotropic transition ($T_{N–I}$) at 70 °C. The observed smectic-to-nematic and nematic-to-isotropic transitions are typical for LCs used in commercial LCDs [25]. According to literature [26], their T_g is around –90 °C. However, the glass transition could not be detected in our analysis due to the sensitivity limitations of the DSC instrument, which starts measuring at –80 °C.

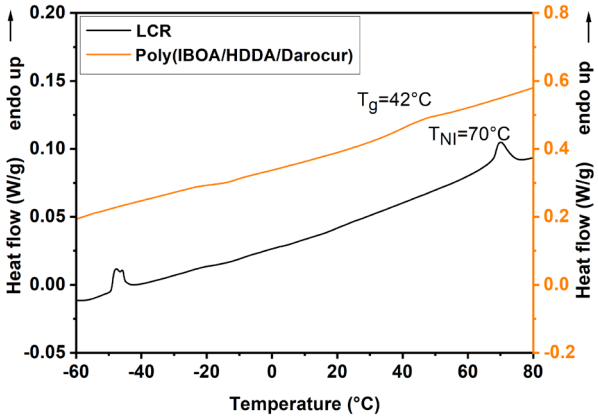

Fig. 2. Thermogrammes obtained by DSC of poly (IBOA/HDDA/Darocur) and LCRs.

Pure poly(IBOA/HDDA/Darocur) shows a T_g close to 47 °C, which is in agreement with previously reported values for this polymer [14]. In the case of the poly(IBOA/HDDA/Darocur) LCR composites, T_{N-I} was not observed. This absence is attributed to the encapsulation of the LCR molecules within the polymer network during curing, which limits their mobility and prevents the mesophase transitions typically observed in LCRs. The suppression of these transitions indicates good dispersion and encapsulation of the LCRs within the polymer matrix. The absence of mesophase transitions in these composite systems suggests that the polymer network effectively restricts the movement of the LCR molecules, resulting in their physical confinement. This confinement and restriction is essential for the design of PDLCs. PDLCs typically rely on the ability of LCs to reorient under an electric field, thereby changing their optical properties [27-30]. However, in the case of our composite systems, encapsulation

within a rigid polymer network may restrict the ability of LCs to freely reorient, which could reduce the electro-optical response of the material.

Nevertheless, the limited mobility of the LCRs within the polymer matrix could still offer promising applications for passive PDLC systems, where the LCs remain in a dispersed, randomly oriented state in the absence of an applied electric field. This property could be particularly advantageous for applications such as smart windows or privacy screens, where the material undergoes transitions between opaque and transparent states in response to external stimuli such as electric fields, temperature, or light exposure [31-32].

The suppression of mesophase transitions and the confinement of LCRs in the polymer network also suggest that these composites could be tailored for applications requiring controlled optical switching, where precise manipulation of LCR alignment and dispersion within the polymer is key. Further optimization of the polymer matrix, such as adjusting the crosslinking density or using different photoinitiators, could allow fine-tuning of the electro-optical response and thus improve the performance of PDLC-based devices.

3.3. Dynamic Mechanical Analysis

To examine the influence of the cross-linking agent on T_g and the network structure, DMA was used to analyze samples containing IBOA monomer with varying concentrations of HDDA (0.1 wt%, 1 wt%, and 2 wt%) and 0.5 wt% Darocur.

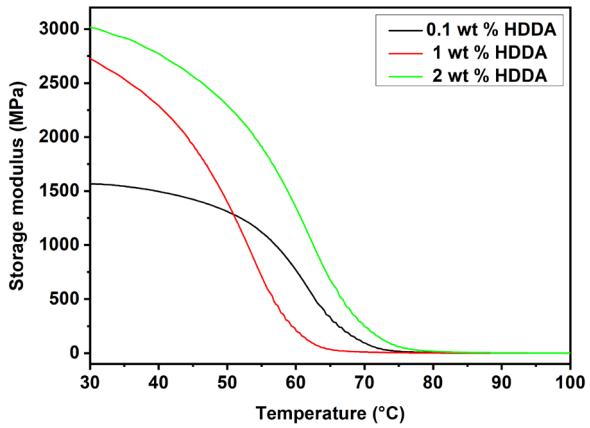

Fig. 3. The storage modulus E' of Poly(IBOA/HDDA/Darocur) in the presence of 0.5 wt% Darocur as a function of HDDA concentration.

Fig. 3 shows the evolution of E′ as a function of temperature for the three HDDA concentrations. Initially, the storage modulus is high and decreases with increasing temperature until the rubbery plateau is reached. The observed decrease in E′ at lower HDDA concentrations highlights the importance of network

density: higher HDDA levels result in a more cross-linked, rigid structure that resists thermal softening [33].

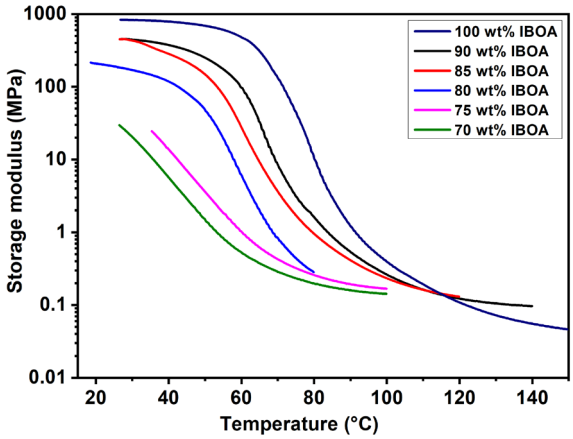

Fig. 4. Storage modulus E' of LCR/poly(IBOA/HDDA/Darocur) mixtures as a function of temperature.

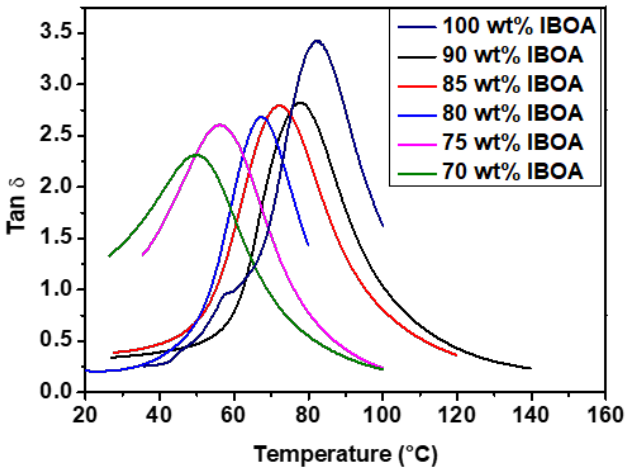

Fig. 5. The variation of tan (δ) of LCR/poly(IBOA/HDDA/Darocur) mixtures as a function of temperature.

To further investigate the influence of LCRs on the T_g of poly(IBOA/HDDA/Darocur), several samples were prepared with different LCR concentrations while keeping Darocur and HDDA at 0.5 wt%. Fig. 4 shows the temperature dependent storage modulus for these blends. The pure poly(IBOA/HDDA/Darocur) system shows the highest modulus (~1000 MPa), reflecting a well-developed crosslinked network. With increasing LCR content, the storage modulus decreases significantly, reaching ~50 MPa for the 70 wt% poly(IBOA/HDDA/Darocur)/30 wt% LCR sample. This behavior is characteristic

of a plasticizing effect, where the LCRs act as flexible, low-T_g additive that interfere with chain packing and reduce intermolecular interactions, thereby softening the polymer matrix [34-35].

The evolution of tan δ as a function of temperature is shown in Fig. 5 for the LCR/poly(IBOA/HDDA/Darocur) blends. The peak of the tan δ curve corresponds to the T_g of the polymer matrix. As the LCR content increases, this peak shifts to lower temperatures, clearly indicating a decrease in T_g. This trend supports the conclusion that LCRs disrupt the segmental motion of the polymer chains, acting as internal plasticizers and lowering the temperature at which the glass-rubber transition occurs [36-37].

Fig. 5 demonstrates a steady decline in T_g as the LCR content increases, indicating a reduction in network rigidity due to lower crosslinking efficiency in the presence of LCRs. This may be due to phase incompatibility or partial miscibility affecting the homogeneous formation of crosslinked domains. The combined decrease in storage modulus and T_g with higher LCR loading reveals a systematic weakening of the polymer network, but also offers a method to tune the mechanical flexibility, which can be advantageous in applications such as soft actuators, optical elastomers or flexible displays [38-39].

3.4. Rheology analysis

Fig. 6 illustrates the modulus (G′) of LCR/poly(IBOA/HDDA/Darocur) blends over a range of polymer concentrations, from 100 wt% to 20 wt% poly(IBOA/HDDA/Darocur), with 0.5 wt% HDDA and 0.5 wt% Darocur held constant.

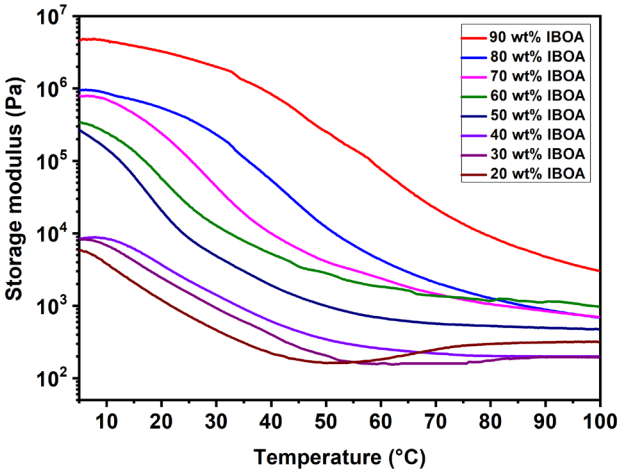

Fig. 6. The variation of the elastic modulus G' as a function of temperature for different concentrations of poly(IBOA/HDDA/Darocur).

The pure poly(IBOA/HDDA/Darocur) system exhibits a high modulus of

elasticity of approximately 100,000 MPa, characteristic of a densely cross-linked rigid thermoset. This value serves as a benchmark that separates two behavioral regimes. Formulations with more than 50 wt% poly(IBOA/HDDA/Darocur) retain high G′ values, reflecting robust network formation, while compositions with increasing LCR content show a pronounced drop in G′, indicating progressive softening due to reduced network stiffness.

This decrease in modulus is primarily due to the plasticizing effect of the LCR phase, which interferes with chain entanglement and crosslinking efficiency. LCRs act as low-molecular-weight additives that disrupt the dense polymer network, reduce the effective crosslink density, and increase chain mobility. As a result, the material transitions from a stiff thermoset to a more compliant, elastomer-like system. The steepest decrease in G′ is observed below 50 wt% poly(IBOA/HDDA/Darocur), where the system loses its structural stiffness, an effect that aligns well with design goals for PDLC technologies that require flexibility and electro-optical responsiveness [40].

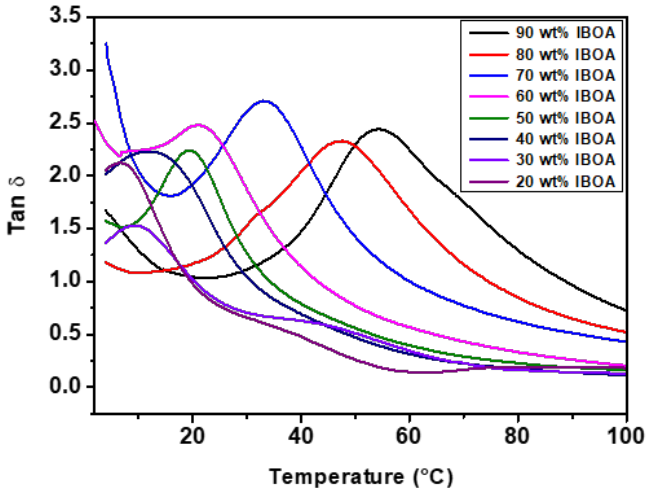

Fig. 7. Variation of the loss factor modulus (tan δ) with temperature for different concentrations of poly (IBOA/HDDA/Darocur).

Fig. 7 shows the tan δ (loss factor) profiles of the same formulations as a function of temperature. The T_g, determined by the peak in tan δ, shows a clear dependence on the LCR content. Pure poly(IBOA/HDDA/Darocur) has a T_g of about 69.6 °C (not shown). As the LCR concentration increases, the T_g decreases non-linearly - initially following a nearly linear decrease, then transitioning to a steeper decrease above ~50 wt% LCR. At the highest LCR concentration (80 wt%), T_g reaches as low as 6.4 °C. This trend confirms the strong plasticizing effect of LCRs, which lower the segmental mobility threshold by disrupting the polymer chain packing and reducing the thermal energy required for glass transition [41].

To validate the T_g behavior, Fig. 8 compares values obtained from DMA and rheological measurements. Both techniques show a decrease in T_g with increasing LCR content, but DMA consistently reports Tg values 10-15°C higher than rheology. This discrepancy can be attributed to differences in deformation modes (tensile/bending for DMA and shear for rheology), instrumental limitations (DMA could not analyze low-T_g samples), and variations in frequency and heating rates [42]. Despite these factors, the results from both methods are qualitatively consistent.

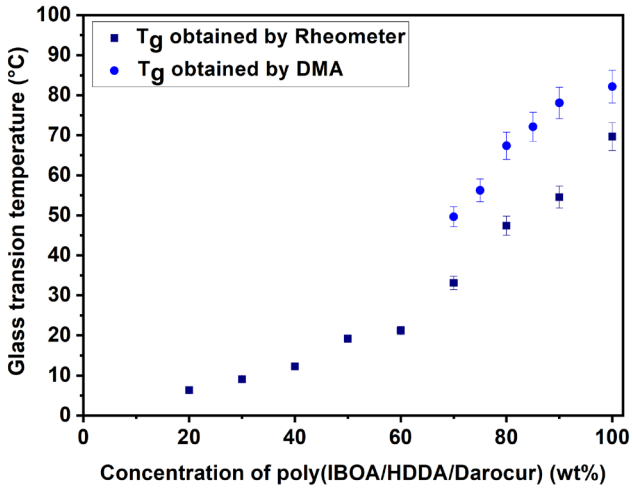

Fig. 8. Superposition of the glass transition temperature of poly (IBOA/HDDA/Darocur)/LCR composites at different concentrations by DMA and rheometer.

In summary, increasing LCR concentration reduces both the elastic modulus and T_g of the blends, transforming the system from a rigid crosslinked network to a soft, thermally responsive matrix. The non-linear decrease in T_g, especially beyond 50 wt% LCR, highlights the strong plasticizing capability of the LC phase. This tunability is essential for PDLC applications where electro-optic functionality depends on material softness and thermal behavior. The consistency between rheological and DMA-derived trends reinforces the robustness of these results and underscores the utility of dual-mode characterization in the evaluation of advanced polymer-LC composites [43-44].

4. Conclusions

This study demonstrates the integration of recycled LC components into UV-curable IBOA-based photopolymers, resulting in materials with tunable thermal and mechanical properties. Physical characterization revealed that radical crosslinking reactions led to high monomer-to-polymer conversion (FTIR), and DSC showed suppression of mesophase transitions, indicating confinement of mesogens within the polymer matrix. DMA data showed a decrease in storage

modulus and T_g with increasing LC content, suggesting plasticization effects that enhance chain mobility and reduce crosslink density. Rheology further confirmed these effects by indicating lower viscosity and improved flow in the uncured state, suggesting better processability. These results highlight the role of recycled mesogenic additives in modulating molecular architecture, phase behavior, and viscoelastic properties. This work also introduces a sustainable approach to designing polymer composites with controlled mechanical and thermal properties, suitable for applications in optical systems, smart windows, and soft photonic devices.

Acknowledgments

This research benefited from the fruitful collaboration between the LRM laboratory at UABB, LPCMCE at USTO-MB, and UMET at the University of Lille, within the framework of the Hubert Curien Program (PHC Tassili). We express our sincere gratitude to all individuals and teams who contributed to the success of this project. Our thanks extend to the Algerian Ministry of Higher Education and Scientific Research (MESRS), the General Directorate of Scientific Research and Technological Development (DGRSDT) of Algeria, as well as the Universities of Tlemcen and USTO-MB/Algeria. We also acknowledge the financial and logistical support provided by CNRS and the University of Lille, France.

R E F E R E N C E S

[1]. *A. Vishwakarma, S. Hait*, E-Waste Valorization and Resource Recovery. In Management of Electronic Waste, A. Priya (Ed.), Wiley, 2024

[2]. *R. Ahirwar, A.K. Tripathi*, E-waste management: A review of recycling process, environmental and occupational health hazards, and potential solutions, Environmental Nanotechnology, Monitoring & Management, **vol. 15**, 2021, 100409

[3]. *J. Cui, N. Zhu, Y. Li, D. Luo, P. Wu, Z. Dang*, Rapid and green process for valuable materials recovery from waste liquid crystal displays, Resources, Conservation and Recycling, **vol. 153**, 2020, 104544

[4]. *A. Barrera, C. Binet, F. Danede, J.F. Tahon, B. Ouddane, F. Dubois, P. Supiot, C. Foissac, U. Maschke,* Chemical Characterization and Thermal Analysis of Recovered Liquid Crystals, Crystals, **vol. 13**, 2023, 1064

[5]. *I. Moundoungou, Z. Bouberka, G.J. Fossi Tabieguia, A. Barrera, Y. Derouiche, F. Dubois, P. Supiot, C. Foissac, U. Maschke*, End-of-Life Liquid Crystal Displays Recycling: Physico-Chemical Properties of Recovered Liquid Crystals, Crystals, **vol. 12**, 2022, 1672

[6]. *A. Barrera, C. Binet, F. Dubois, P.A. Hébert, P. Supiot, C. Foissac, U. Maschke*, Temperature and frequency dependence on dielectric permittivity and electrical conductivity of recycled Liquid Crystals, Journal of Molecular Liquids, **vol. 378**, 2023, 121572

[7]. *C.H. Han, J.H. Lee, C.H. An, S.W. Oh*, A liquid crystal smart window for energy saving and harvesting, Applied Materials Today, **vol. 35**, 2023, 101923

[8]. *F. Dong, Y. Qian, X. Xu, H. Shaghaleh, L. Guo, H. Liu, S. Wang*, Preparation and characterization of UV-curable waterborne polyurethane using isobornyl acrylate modified via copolymerization, Polymer Degradation and Stability, **vol. 184**, 2021, 109474

[9]. *A. Uddin, S. Allen, A. Rylski, C. O'Dea, J. Ly, T. Grusenmeyer, S. Roberts, Z. Page*, Do The Twist: Efficient Heavy-Atom-Free Visible Light Polymerization Facilitated by Spin-Orbit Charge Transfer Inter-system Crossing, Angewandte Chemie International Edition, **vol. 62**, 2023, e202219140

[10]. *E.S. Kim, J.H. Lee, D.H. Suh, W.J. Choi,* Influence of UV Polymerization Curing Conditions on Performance of Acrylic Pressure Sensitive Adhesives, Macromolecular Research, **vol. 29**, 2021, pp. 129–139

[11]. *R. Anastasio, R. Cardinaels, G.W.M. Peters, L.C.A. van Breemen*, Structure–mechanical property relationships in acrylate networks, Applied Polymer Science, **vol. 137**, 2020, app.48498

[12]. *E. Andrzejewska*, Photopolymerization kinetics of multifunctional monomers, Progress in Polymer Science, **vol. 26**, 2001, pp. 605–665

[13]. *S. Salkhi Khasraghi, A. Shojaei, U. Sundararaj*, Bio-based UV curable polyurethane acrylate: Morphology and shape memory behaviors, European Polymer Journal, **vol. 118**, 2019, pp. 514-527

[14]. *N. Zeggai, B. Dali Youcef, F. Dubois, T. Bouchaour, P. Supiot, L. Bedjaoui, U. Maschke*, Analysis of dynamic mechanical properties of photochemically crosslinked poly(isobornylacrylate-co-isobutylacrylate) applying WLF and Havriliak-Negami models, Polymer Testing, **vol. 72**, 2018, pp 432-438

[15]. *H. Lin, Y. Zhao, X. Jiao, H. Gao, Z. Guo, D. Wang, Y. Luan, L. Wang,* Preparation and Application of Polymer-Dispersed Liquid Crystal Film with Step-Driven Display Capability, Molecules, **vol. 29**, 2024, 1109

[16]. *A.L. Qin, B. Yan, C. Zhang, Y.H. Wang,* Effect of concentration of macro-initiator and crosslinking agent on electro-optical properties of polymer dispersed liquid crystal. Gaofenzi Cailiao Kexue Yu Gongcheng/Polymeric Materials Science and Engineering, **vol. 25**, 2009, pp. 96-99

[17]. *Z.C. Jiang, Q. Liu, Y.Y. Xiao, Y. Zhao*, Liquid crystal elastomers for actuation: A perspective on structure-property-function relation, Progress in Polymer Science, **vol. 153**, 2024, 101829

[18]. *J.V. Crivello*, UV Curing: Science and Technology (Ed. S. Peter Pappas), pp. 24–77, Technology Marketing Corporation, 1978

[19]. *J.P. Fouassier, J. Lalevée*, "Photoinitiators for Polymer Synthesis," Wiley-VCH, 2012.

[20]. *G. Odian*, *Principles of Polymerization*, 4th ed., Wiley, 2004

[21]. *S. Agarwal, S. Srivastava, S. Joshi, S. Tripathi, B. Pratap Singh, K. Kumar Pandey, R. Manohar*, A Comprehensive Review on Polymer-Dispersed Liquid Crystals: Mechanisms, Materials, and Applications, ACS Materials Au, **vol. 5**, 2025, pp. 88-114

[22]. *R. Bhargava, S.Q. Wang, J.L. Koenig*, Studying Polymer-Dispersed Liquid-Crystal Formation by FTIR Spectroscopy. 1. Monitoring Curing Reactions, Macromolecules **vol. 32**, 1999, pp. 8982–8988

[23]. *D.L. Pavia, G.M. Lampman, G.S. Kriz, J.R. Vyvyan*, Introduction to Spectroscopy. 5th ed. Cengage Learning, 2014

[24]. *G. Socrates*, Infrared and Raman Characteristic Group Frequencies: Tables and Charts. 3rd ed. Wiley, 2001

[25]. *N.A. Vaz, G.W. Smith, G.P. Montgomery,* A Light Control Film Composed of Liquid Crystal Droplets Dispersed in a UV-Curable Polymer. Molecular Crystals and Liquid Crystals, **vol. 146**, 1987, pp. 1–15

[26]. *A. Barrera, C. Binet, F. Dubois, P.A. Hébert, P. Supiot, C. Foissac, U. Maschke*, Recycling of liquid crystals from e-waste. Detritus, **vol. 21**, 2022, pp. 55–61

[27]. *D. Manaila-Maximean*, Confined liquid crystals - polymer dispersed liquid crystal films, UPB Scientific Bulletin, Series A: Applied Mathematics and Physics, **vol. 83**, 2021, pp. 271-278

[28]. *D. Manaila-Maximean*, Materiale composite cu cristale lichide (Composite materials with liquid crystals), Ed. Printech, Bucharest, 2008

[29]. *D. Manaila-Maximean, R. E. Bena*, Cristale lichide in optoelectronica (Liquid crystals in optoelectronics), Ed. Politehnica Press, Bucharest, 2011

[30]. *D. Manaila-Maximean, C. P. Ganea, V.A. Loiko, A.V. Konkolovich, V. Cîrcu, O. Dănilă, A. Bărar*, "Polymer dispersed liquid crystals doped with nanoparticles: electric and electro-optical properties", (SPIE) Conference Series, In Advanced Topics in Optoelectronics, Microelectronics and Nanotechnologies X **vol. 11718**, pp. 117182R-117188, 2020

[31]. *H. Zhang, Z. Miao, W. Shen*, Development of polymer-dispersed liquid crystals: From mode innovation to applications, Composites Part A: Applied Science and Manufacturing, **vol. 163**, 2022, 107234

[32]. *C. Sen, B. Alkan, O. Mohammadmoradi, A. Taralp*, Polymer Dispersed Liquid Crystal Smart Film Technologies: Overview. IntechOpen, 2024

[33]. *L.H. Sperling*, Introduction to Physical Polymer Science, 4th ed., Wiley, 2006

[34]. *M. Baiardo, G. Frisoni, M. Scandola, M. Rimelen, D. Lips, K. Ruffieux, E. Wintermantel*, Thermal and mechanical properties of plasticized poly (L-lactic acid), Journal of Applied Polymer Science, **vol. 90**, 2003, p. 1731

[35]. *F. Benmouna, U. Maschke, X. Coqueret, M. Benmouna*, Equilibrium phase behavior of polymer and liquid crystal blends, Macromolecular Theory and Simulations, **vol. 9**, 2000, pp. 215-229

[36]. J.G. Drobny, Handbook of Thermoplastic Elastomers, 2nd ed., William Andrew Publishing, 2014

[37]. *J.D. Badia, L. Santonja-Blasco, A. Martínez-Felipe, A. Ribes-Greus*, Dynamic Mechanical Thermal Analysis of Polymer Blends. In Characterization of Polymer Blends (eds S. Thomas, Y. Grohens and P. Jyotishkumar), Wiley, 2014

[38]. *I.C. Khoo, S.T. Wu*, Optics and Nonlinear Optics of Liquid Crystals, World Scientific, 1993

[39]. *W. Jeu*, Liquid Crystal Elastomers: Materials and Applications, Edited by Wim H. de Jeu. Advances in Polymer Science, vol. 250, Springer Verlag, 2012

[40]. *H.S. Hakemi*, Electro-optical performances of flexible polymer dispersed liquid crystals as a function of liquid crystal concentration. Trends in Technical & Scientific Research , **vol 7**, 2023, 555704

[41]. *F. Benmouna, A. Daoudi, F. Roussel, L. Leclercq, J.M. Buisine, X. Coqueret, M. Benmouna, B. Ewen, U. Maschke*, Effect of Molecular Weight on the Phase Diagram and Thermal Properties of Poly(styrene)/8CB Mixtures, Macromolecules, **vol. 33**, 2000, pp. 960 – 967

[42]. *M. Isreb, M. Chalkia, T. Gough, R.T. Forbes, P. Timmins*, A Combined Rheological and Thermomechanical Analysis Approach for the Assessment of Pharmaceutical Polymer Blends. Polymers, **vol. 14**, 2022, 3527

[43]. *H. Kihara, R. Kishi, T. Miura, S. Horiuchi, Y. Okada, K. Yase, H. Ichijo*, Thermomechanical analysis of a polymer dispersed liquid crystal containing a thermoplastic elastomer, Liquid Crystals, **vol. 28**, 2001, pp. 1655-1658

[44]. *Z. Liu, H. Wang, C. Zhou*, Synthesis and Characterization of a Liquid Crystal-Modified Polydimethylsiloxane Rubber with Mechanical Adaptability Based on Chain Extension in the Process of Crosslinking, ACS Omega, **vol. 7**, 2022, pp. 36590-36597